A role for the ELAV RNA-binding proteins in neural stem cells: stabilization of *Msi1* mRNA

Antonia Ratti[1,*], Claudia Fallini[1], Lidia Cova[1], Roberto Fantozzi[1], Cinzia Calzarossa[1], Eleonora Zennaro[1], Alessia Pascale[2], Alessandro Quattrone[3] and Vincenzo Silani[1]

[1]Department of Neuroscience, 'Dino Ferrari' Centre, University of Milan–IRCCS Istituto Auxologico Italiano, Via Zucchi 18, 20095 Cusano Milanino, Italy
[2]Department of Experimental and Applied Pharmacology, University of Pavia, Via Taramelli 14, 27100 Pavia, Italy
[3]Laboratory of Metabolomics and Systems Biology, Magnetic Resonance Center and FiorGen Foundation, University of Florence, Via Sacconi 6, 50019 Sesto Fiorentino, Italy
*Author for correspondence (e-mail: antonia.ratti@unimi.it)

Accepted 21 December 2005
Journal of Cell Science 119, 1442-1452 Published by The Company of Biologists 2006
doi:10.1242/jcs.02852

Summary

Post-transcriptional regulation exerted by neural-specific RNA-binding proteins plays a pivotal role in the development and maintenance of the nervous system. Neural ELAV proteins are key inducers of neuronal differentiation through the stabilization and/or translational enhancement of target transcripts bearing the AU-rich elements (AREs), whereas Musashi-1 maintains the stem cell proliferation state by acting as a translational repressor. Since the gene encoding Musashi-1 (*Msi1*) contains a conserved ARE in its 3′ untranslated region, we focused on the possibility of a mechanistic relationship between ELAV proteins and Musashi-1 in cell fate commitment. Colocalization of neural ELAV proteins with Musashi-1 clearly shows that ELAV proteins are expressed at early stages of neural commitment, whereas interaction studies demonstrate that neural ELAV proteins exert an ARE-dependent binding activity on the *Msi1* mRNA. This binding activity has functional effects, since the ELAV protein family member HuD is able to stabilize the *Msi1* ARE-containing mRNA in a sequence-dependent way in a deadenylation/degradation assay. Furthermore activation of the neural ELAV proteins by phorbol esters in human SH-SY5Y cells is associated with an increase of Musashi-1 protein content in the cytoskeleton. We propose that ELAV RNA-binding proteins exert an important post-transcriptional control on Musashi-1 expression in the transition from proliferation to neural differentiation of stem/progenitor cells.

Supplementary material available online at
http://jcs.biologists.org/cgi/content/full/119/7/1442/DC1

Key words: ELAV, Musashi-1, Neurogenesis, RNA-binding protein, Stem cell

Introduction

In mammals, adult neurogenesis was demonstrated to be active in two main brain regions, namely the subventricular zone (SVZ) and the dentate gyrus of the hippocampus, where neural stem cells (NSCs) were isolated (Alvarez-Buylla and Garcia-Verdugo, 2002; Galli et al., 2003). NSCs are characterized by plasticity and multipotency so that they may proliferate and/or undergo differentiation into functional progeny according to the environmental conditions (Bottai et al., 2003). These features make them ideal candidate targets for the cure of neurodegenerative diseases, although the molecular mechanisms that determine a NSC to proliferate or to differentiate towards a neuronal or astroglial fate are only partially elucidated (Qian et al., 2000; Roegiers and Jan, 2004). Post-transcriptional regulation, exerted by RNA-binding proteins (RBPs) as an alternative mechanism to the activity of transcription factors in modulating gene expression, has recently been shown to have a role in the development of the central nervous system (CNS) and, in particular, in the control of the NSC division mode (Okano et al., 2002). Several neural-specific RBPs have been described so far to affect splicing, transport, translation and stability of target mRNAs, and can cause severe neurological disorders when altered (Perrone-Bizzozero and Bolognani, 2002).

The Musashi-1 (Msi1) RBP was first reported to be required for the proper development of the neural sensory organ in *Drosophila* (Nakamura et al., 1994), whereas in mammals it is commonly considered a specific marker for stem/progenitor cells of neural origin (Kaneko et al., 2000; Maslov et al., 2004). Msi1 acts as a translational suppressor by binding to the 3′-untranslated region (3′UTR) of specific mRNA targets. In this way the proliferation state of NSCs is maintained by inhibiting the translation of the membrane protein Numb, involved in the Notch/Delta signaling cascade (Imai et al., 2001), and of the cyclin-dependent kinase inhibitor $p21^{WAF-1}$ (Battelli et al., 2006).

The neuronal-specific ELAV (nELAV) RBPs, which are associated with the pathological condition of paraneoplastic encephalomyelitis (Szabo et al., 1991), are necessary and sufficient to induce neuronal differentiation in mammalian cells (Akamatsu et al., 1999; Kasashima et al., 1999), as is their *elav* ortholog in *Drosophila* (Robinow and White, 1991). The three mammalian nELAV family members, HuB, HuC and HuD, are commonly referred to as early and specific markers

Journal of Cell Science

Journal of Cell Science

of post-mitotic neurons during CNS development (Barami et al., 1995; Okano and Darnell, 1997; Wakamatsu and Weston, 1997), whereas the fourth member, HuR, is ubiquitously expressed. The ELAV RNA-binding activity promotes the stabilization and/or translation of an array of transcripts containing the AU-rich consensus element (ARE) in their 3′UTR (Antic and Keene, 1997). ARE sequences represent well-documented cis-acting regulatory motifs usually identified in mRNAs of genes with a high turnover rate (Shaw and Kamen, 1986), and are recognized by several ARE-binding proteins which exert a different and often opposite role on mRNA fate (Bevilacqua et al., 2003). nELAV target genes are endowed with a wide variety of biological functions (Gao et al., 1994), from cell growth regulation (Levine et al., 1993) to brain maturation and maintenance (Antic et al., 1999; Aranda-Abreu et al., 1999; Chung et al., 1997).

The expression of Msi1 and nELAV RBPs has been initially described to be spatiotemporally sequential during the development of murine CNS (Sakakibara et al., 1996), although recent data suggest that nELAV proteins might have an important role as early as the neuronal-specific commitment of NSCs (Akamatsu et al., 2005).

In the present work we show that nELAV proteins are expressed and colocalize with Msi1 in the adult mouse SVZ and in cultured NSCs/progenitors, where they show a specific and ARE-dependent binding activity for the *Msi1* transcript. In particular, we find that nELAV RBPs exert a stabilizing activity on *Msi1* mRNA decreasing its turnover rate in vitro and promoting its translation in vivo. Such findings suggest a mechanistic correlation between nELAV and Msi1 RBPs in controlling the proliferation/differentiation activities of neural stem/progenitor cells.

Results

The mammalian *Msi1* 3′UTR contains a conserved AU-rich element which is bound by multiple RBPs including the nELAV proteins

Examination of the mouse *Msi1* gene revealed the presence of a putative ARE consensus sequence in its 3′UTR, catalogued as belonging to group III in the ARE-mRNA database (ARED) (Bakheet et al., 2001). Since AREs are cis-acting regulatory sites, they are usually well conserved throughout phylogenesis (Asson-Batres et al., 1994), and indeed a comparative analysis of *Msi1* 3′UTRs in ortholog genes revealed that the human sequence showed a 75% identity with its murine counterpart (Fig. 1A). The EST-expanded rat *Msi1* 3′UTR displayed the same degree of conservation (74%), and alignment of the three sequences gave almost full identity of a region of 24 bp, including the putative functional ARE. On the other hand, *Danio rerio*, *Xenopus laevis*, *Caenorhabditis elegans* and *Drosophila melanogaster* Msi1 orthologs neither contained the ARE signature nor showed any significant homology along the entire 3′UTR region. Also *Msi2* gene, the ubiquitously expressed member of the Musashi family (Sakakibara et al., 2001), didn't show any ARE consensus sequence in its 3′UTR. Therefore, we hypothesized that the ARE sequence present in the *Msi1* gene could have a role in influencing its mRNA stability and in the post-transcriptional regulation of its expression only in mammals. Prediction of the mouse *Msi1* 3′UTR secondary structure by the Sfold RNA-folding algorithm (Ding et al., 2004) clearly showed that the ARE sequence is exposed in a single-stranded loop, which is likely to be accessible to ARE-binding proteins (Fig. 1B).

In order to investigate the putative RNA-binding activities associated with the *Msi1* transcript, we performed RNA/protein UV crosslinking experiments in the presence of radiolabeled *Msi1* 3′UTR riboprobe and protein extracts from both mouse brain and cultured NSCs. After UV irradiation, the resulting mRNA-protein (mRNP) complexes were separated by SDS-PAGE and the electrophoretic pattern was compared with that obtained for the growth-associated protein 43 (*Gap43*), a well-known mRNA target of the nELAV RBPs. A partially overlapping profile was evident with common bands of approximately 95, 65 and 42 kDa (Fig. 1C), the latter being previously shown to correspond to the RNA-binding activity of HuD (Chung et al., 1997). We observed two additional mRNP complexes specific to the *Msi1* 3′UTR, with apparent molecular weights of 37 and 32 kDa, the lower band being more abundant in NSCs and the upper one in whole brain lysate.

These preliminary findings prompted us to investigate the possible role of the nELAV RBPs as trans-acting factors in the binding and regulation of the *Msi1* transcript. To this purpose after UV crosslinking assays, the resulting mRNP complexes were immunoprecipitated with the pan anti-nELAV antibody (16A11), which is known to recognize the three neuronal RBPs HuB, HuC and HuD, but not HuR (Marusich et al., 1994) (Fig. 1D). A 42 kDa complex was immunoprecipitated in the presence of the *Msi1* 3′UTR riboprobe, confirming the existence of an nELAV RNA-binding activity for the *Msi1* transcript both in mature brain and in NSCs.

As several RBPs are reported to bind to their own mRNA (Chu et al., 1991; Schaeffer et al., 2001), including nELAV proteins (Abe et al., 1996; Samson, 1998), we also immunoprecipitated the products of the UV crosslinking reaction using the anti-Msi1 antibody, but the *Msi1* transcript was not recovered (Fig. 1E).

nELAV proteins are expressed in neural stem/progenitor cells in vitro

Our preliminary data suggest the existence of a functional correlation between the *Msi1* gene, associated with the maintenance of NSC proliferation, and the nELAV RBPs, usually considered early markers of newly generated neurons. NSCs isolated from developing or mature brain can be grown in vitro as floating cell aggregates denominated neurospheres, which are characterized by an indefinite proliferation potentiality and by the multipotency to differentiate into the principal neural phenotypes (Morshead and van der Kooy, 2004). We therefore looked for nELAV protein expression in neurospheres obtained from adult mouse brains. Immunolabeling images with the anti-Msi1 antibody showed colocalization with the nELAV antigens throughout the sphere (Fig. 2A-C), suggesting a stem identity of nELAV-positive cells. To further characterize the expression of these RBPs, from tridimensional neurospheres we obtained a monolayer of stem/progenitor cells after dissociation and exposure to adhesive substrate for 1 hour. This limited period of time allows the preservation of the typical NSC heterogeneous morphologies and it is not sufficient to commit cells towards a specific fate (Bez et al., 2003; Suslov et al., 2002). As in neurosphere cultures, double fluorescent signals for nELAV

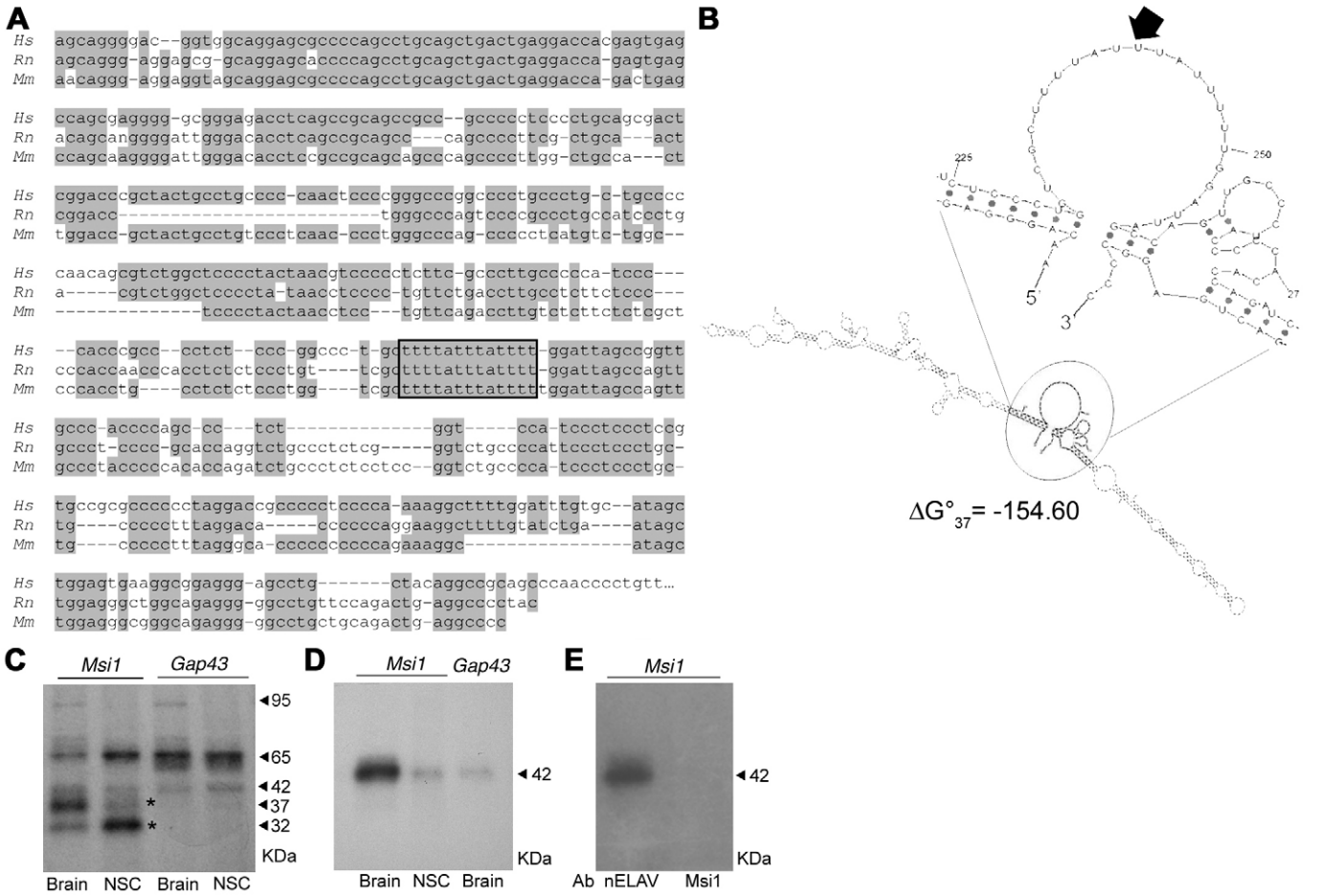

Fig. 1. Computational analysis of the *Msi1* 3′UTR sequence and identification of the associated RBP activities. (A) Alignment of the mammalian *Msi1* 3′UTR sequences is shown: *Homo sapiens* (*Hs*, NM_002442) at the top, *Rattus norvegicus* (*Rn*, CD568097) in the middle and *Mus musculus* (*Mm*, NM_008629) at the bottom. Conserved nucleotides are highlighted in grey, whereas the ARE is indicated by the box. (B) The most stable RNA secondary structure of the mouse *Msi1* 3′UTR as predicted by the Sfold software (www.bioinfo.rpi.edu). The magnification shows the loop exposing the ARE sequence, indicated by the arrow. (C) UV crosslinking assay of *Msi1* and *Gap43* 3′UTR riboprobes and lysates from whole mouse brain and NSCs. The 95 kDa complex is detected only when brain extracts were used. The 37 and 32 kDa RNA-binding activities specific for *Msi1* sequence are indicated by asterisks. (D) Immunoprecipitation of *Msi1* and *Gap43* riboprobes with the anti-nELAV antibody after UV irradiation on brain and NSC extracts. A 42 kDa complex (arrowhead) was precipitated in all samples. (E) Immunoprecipitation of the NSC UV crosslinked mRNPs with the anti-nELAV and the anti-Msi1 antibodies, respectively.

and Msi1 were still present although their cellular distribution appeared slightly different, Msi1 signals being prevalent in the nuclei and nELAV RBP signals more diffuse in the cytoplasm (Fig. 2D-F). Coexpression of the intermediate filament nestin, widely used as a neural stem/progenitor cell marker (Wiese et al., 2004), with both nELAV and Msi1 demonstrated the still undifferentiated and proliferating state of our neurosphere-derived cell culture (data not shown). The specificity of the anti-Msi1 antibody used was previously verified in committed progenitor cells with neuronal morphology, which resulted positive for the differentiation marker β-tubulinIII and negative for Msi1, and in immature astrocytes, positive for both GFAP and Msi1 (Sakakibara et al., 1996) (data not shown).

Furthermore, the uncommitted mitotic state of the neurosphere-derived cells was attested by the positive labeling for the proliferation-associated antigen Ki67, a protein produced in all active phases of the cell cycle, but absent in G_0 (Kee et al., 2002). nELAV RBPs and Ki67 were co-expressed in actively proliferating cells with a distinct cellular distribution, nuclear for Ki67 and mainly cytoplasmic for nELAV proteins (Fig. 2G-I). nELAV protein staining was also present in non-proliferating Ki67-negative cells.

nELAV RBPs are expressed in the neurogenic SVZ in vivo

Since our immunostaining data clearly indicate that nELAV proteins are not limited to early post-mitotic and mature neurons, we wanted to investigate nELAV expression in vivo in the SVZ region, one of the germinal areas where neurogenesis occurs in the adult. Brain sections from adult rats were immunolabeled with anti-nELAV and anti-Ki67 antibodies (Fig. 3A,B): nELAV proteins were clearly expressed in the SVZ and overlapped the Ki67 fluorescent signals with a complementary intracellular distribution pattern (Fig. 3C,D). As neuronal-specific markers, nELAV proteins were also strongly expressed in the cerebral areas surrounding the lateral

Journal of Cell Science

ventricle, where Ki67 labeling was absent. Immunostaining with the anti-Msi1 antibody confirmed the presence of stem/progenitor cells in the SVZ. The concomitant expression of Msi1 and nELAV proteins in this neurogenic region (Fig. 3E-G), mainly confined to the sub-ependymal cell layer (Fig. 3H), suggests the importance of both these RBPS in regulating NSC proliferation.

The *Msi1* mRNA is a target of the nELAV proteins in neurospheres

We have found that nELAV proteins are endowed with an RNA-binding activity for the *Msi1* transcript and are expressed in neural stem/progenitor cells in vitro and in vivo. A ribonomic approach (Tenenbaum et al., 2002) was then used to isolate nELAV-containing mRNP complexes from adult mouse neurospheres. Endogenous mRNPs were immunoprecipitated from neurosphere lysates with anti-nELAV, with an irrelevant isotype-matched antibody (anti-His_5) and with no antibody, respectively, in three independent experiments. Precipitated mRNAs from each sample were subjected to quantitative real-time RT-PCR using specific sets of primers for *Msi1*, *Rpl10a*, *Gap43* and *Mapt* (microtubule-associated protein tau) genes. The housekeeping *Rpl10a*, encoding a ribosomal large subunit protein, was used as negative control because it does not contain an ARE consensus sequence in its 3′UTR. *Gap43* and *Mapt* are two well-known mRNA targets of nELAV RBPs both in developing and mature neurons. In the nELAV-containing mRNP complexes, *Msi1* mRNA was enriched 62-fold compared with the control sample (anti-His_5) (Fig. 4), whereas *Rpl10a* was absent in all the experimental conditions tested, although its content in the input lysate was 100-fold more abundant than *Msi1* (see Table S1 in supplementary material). Neither *Gap43* nor *Mapt* transcripts were significantly immunoprecipitated from neurospheres by the anti-nELAV antibody, even if these two genes were expressed in the input lysate and were recovered from mRNPs of mouse mature brain (data not shown).

We also immunoprecipitated the endogenous mRNP complexes containing the Msi1 protein in order to test the presence of the *Msi1* transcript itself among its targets. No significant results were found in line with the negative data obtained in UV crosslinking assays and confirming the observation that the *Msi1* 3′UTR sequence does not show any consensus binding site (G/AU_nAGU) for Msi1 (Imai et al., 2001).

The HuD protein shows an ARE-dependent binding activity for the *Msi1* 3′UTR

We then tested whether nELAV protein binding to *Msi1* mRNA was dependent on the presence of the putative ARE consensus sequence. Two deletion transcripts, ARE^+ and ARE^-, were obtained from the mouse *Msi1* 3′UTR sequence (Fig. 5A), where the ARE^+ fragment encompassed the conserved ARE-containing region we identified by phylogenetic analysis. UV-crosslinking assays on neurosphere lysates revealed that the ARE^+ probe showed the same RBP-binding pattern as the full-length *Msi1* 3′UTR, whereas all RNA-protein interactions were abolished when the ARE^- fragment was used (Fig. 5B, left panel). This finding suggests that the presence of RBPs or associated proteins in the *Msi1*-containing mRNP complexes is strictly dependent on the cis-acting regulatory sequence of the ARE region. We have demonstrated that nELAV proteins exhibit an RNA-binding activity for the *Msi1* transcript both in in vitro and in vivo immunoprecipitation assays. In order to further characterize this binding affinity, we expressed a recombinant His-tagged HuD protein and performed UV-crosslinking experiments. RNA-protein complexes formed with the *Msi1* full-length 3′UTR and ARE^+, but not with the ARE^- riboprobe, confirming a strictly ARE-dependent binding activity of the HuD protein (Fig. 5B, right panel). To demonstrate the specificity of such in vitro binding, competition assays were performed using a 100× molar excess of ARE^+ and ARE^- riboprobes

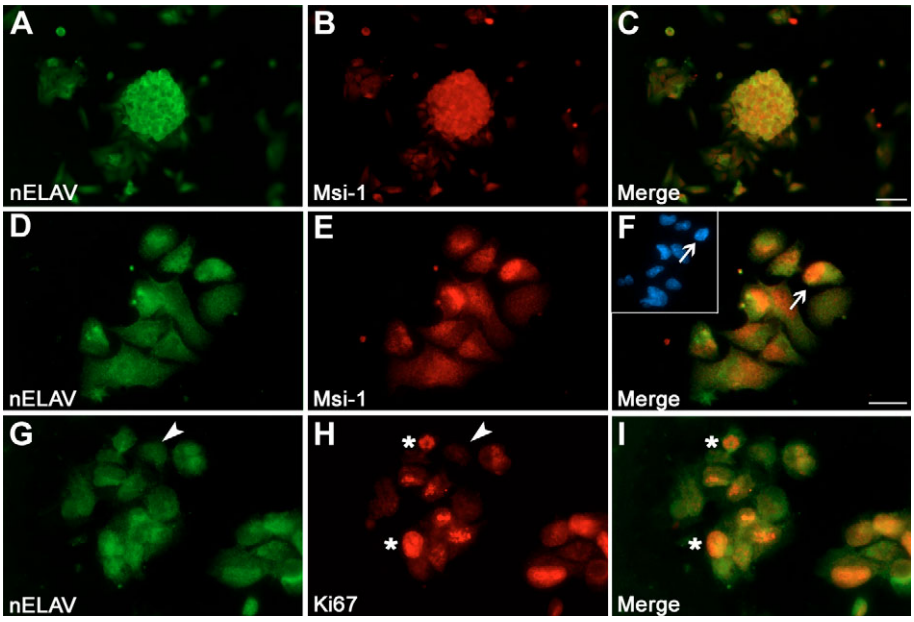

Fig. 2. nELAV RBPs are expressed in neurospheres and neural stem/progenitor cells in vitro. (A,B) The nELAV antibody (green) was used in combination with anti-Msi1 antibody (red) to label adult mouse neurospheres showing a strong overlapping expression of the two RBPs in the whole neurosphere (C, merged). (D,E) Colocalization of nELAV (green) and Msi1 (red) RBPs is more evident in single stem/progenitor cells. Most of the neurosphere-derived precursors show the expression of the two antigens with a different cellular distribution, mainly nuclear for Msi1 (F, merged, arrow). The same field is represented in the inset at a reduced size where nuclei are evidenced by DAPI counterstaining (arrow). (G,H,I) The proliferative state of the cell culture is attested by nELAV (green) and Ki67 (red) positive labeling. These two proteins are coexpressed in certain precursors, whereas nELAV is selectively expressed in others (arrowheads). The nuclear localization of Ki67 antigen is clearly visible (asterisks). Bars, 100 μm (A-C); 25 μm (D-I).

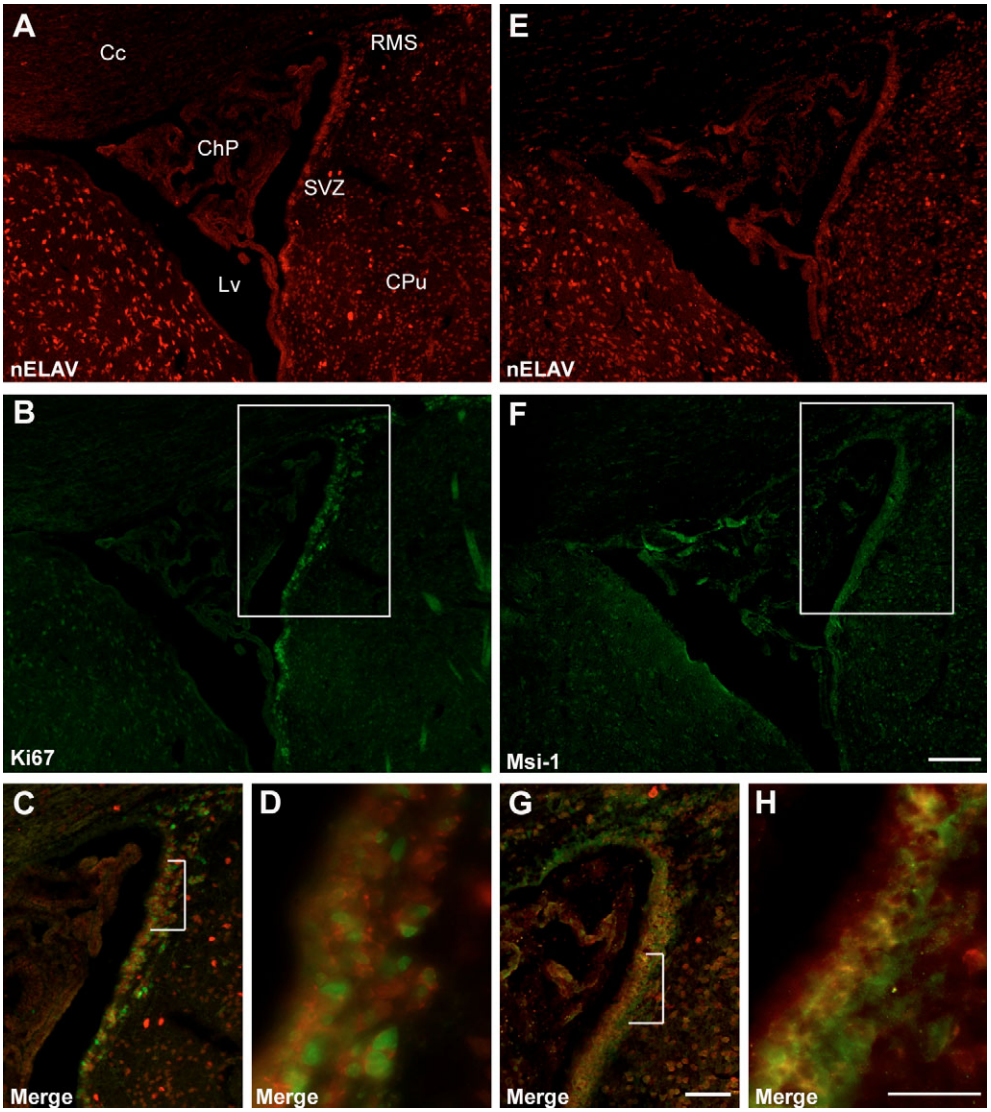

Fig. 3. nELAV proteins are expressed in the proliferating cells of the adult rat SVZ. (A,B) Immunolabeling with anti-nELAV (red) and anti-Ki67 (green) antibodies revealed coexpression of the two markers (C, merged, higher magnification of the field indicated in B) in the sub-ependymal layer of the adult SVZ, where proliferating stem/progenitor cells are present. (D) A magnified image of the region indicated in C (bracket) clearly shows the distinct nuclear and cytoplasmic distribution of the Ki67 and nELAV markers, respectively, in the same cells. (E,F) nELAV (red) and Msi1 (green) RBPs colocalized in the SVZ (G, merged, higher magnification image of the field in F) and presented the same cytoplasmic distribution pattern (H, magnified picture of the region indicated in G by the bracket). Cc, corpus callosus; ChP, choroid plexus; CPu, caudate putamen; Lv, lateral ventricle; RMS, rostral migratory stream. Bars, 100 μm (A,B,E-F); 50 μm (C,G); 25 μm (D,H).

together with *Msi1* full-length 3′UTR (Fig. 5C, left and right panels). Although ARE^{-} had no ability to bind to HuD, cold ARE^{+} and *Msi1* 3′UTR efficiently competed with the radiolabeled probe. The HuD-specific binding to *Msi1* ARE sequence was also confirmed by the absence of interaction with an irrelevant sequence (As). The binding was dose dependent, as shown by UV-crosslinking assays performed with increasing amounts of recombinant HuD protein (Fig. 5D).

HuD acts on the *Msi1* mRNA by reducing its degradation rate

ARE sequence elements are usually present in mRNAs with a high turnover rate (Chen and Shyu, 1995), on which they determine increased or decreased stability, probably depending on the bound RBPs (Lal et al., 2004). We wanted to investigate whether the presence of the HuD-bound ARE in the *Msi1* gene was associated to a cis-acting regulatory role. To this end, the stability profile of the *Msi1* mRNA was studied by means of a functional approach which allowed us to reproduce and follow the mRNA deadenylation/degradation kinetic profile in vitro

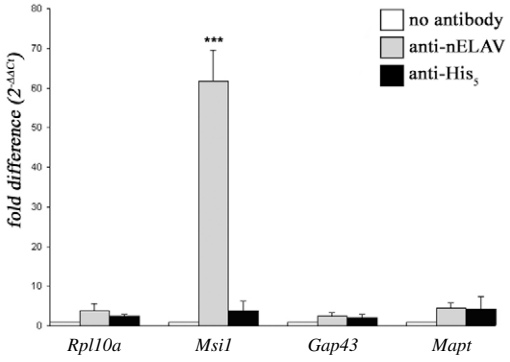

Fig. 4. Real-time PCR-based identification and quantification of mRNAs associated to nELAV-mRNP complexes in adult neurospheres. Endogenous mRNPs were immunoprecipitated by anti-nELAV, anti-His$_5$ and no antibody and the collected mRNA species were quantified by real-time RT-PCR. The normalized fold difference is indicated with respect to the sample where no antibody was used (mean value ± s.e.m.; one-way ANOVA, n=3, ***P<0.001 for anti-nELAV antibody compared with both controls).

Journal of Cell Science

(Ford et al., 1999). For this assay short capped and polyadenylated (polyA$_{60}$) transcripts were synthesized to represent the putative functional region of the *Msi1* 3′UTR. We produced a 114 bp ^{32}P-labeled fragment containing the ARE consensus site (μmsi1ARE^{+}) and an irrelevant 148 bp transcript as a control (μmsi1AS, the antisense sequence of the ARE^{-} fragment). The deadenylation kinetic and the associated degradation of the body of these two synthetic mRNAs, composed only of putative regulatory sequences, were followed by simply visualizing their decrease in length on a denaturing gel. We observed that the deadenylation of the μmsi1ARE^{+} transcript was progressive and became complete within 30 minutes compared with the fully deadenylated probe (A$_0$), used as a reference marker (Fig. 6A). By contrast, high-molecular-weight intermediates of the μmsi1AS probe (i.e. smear length and consistence) were still present after a longer incubation time (45 minutes), indicating a slower degradation kinetic rate.

When the same deadenylation/degradation assay was repeated in the presence of the recombinant HuD protein, the decay rate of the μmsi1ARE^{+} transcript markedly decreased compared with the control, and resembled that of the μmsi1AS mRNA in the degradation profile (Fig. 6B). Indeed, after a 45-minute incubation, the shortening of the polyA$_{60}$ tail was still incomplete compared with the same sample incubated in the absence of HuD, with the persistence of high-molecular-weight species corresponding to the almost intact transcript. When the μmsi1AS mRNA was used, the addition of the recombinant HuD protein did not alter the deadenylation pattern (data not shown). These results demonstrate that the conserved AU-rich region in the *Msi1* 3′UTR acts as a cis-acting regulatory sequence on which the nELAV HuD protein specifically exerts its stabilizing activity by decreasing its mRNA turnover rate.

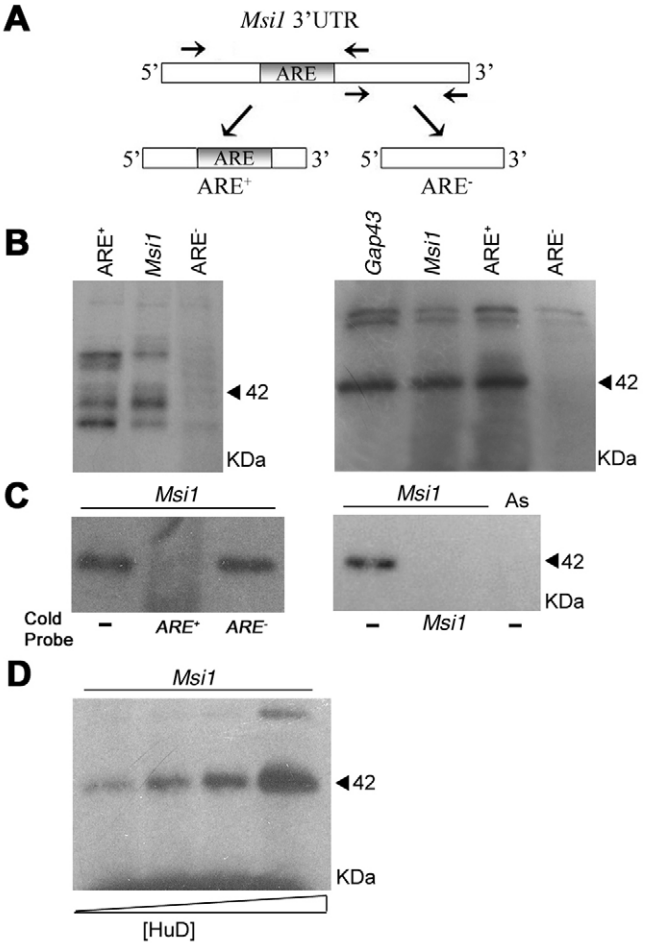

Fig. 5. HuD protein specifically recognizes and binds the *Msi1* 3′UTR sequence. (A) Schematic representation of the mouse *Msi1* 3′UTR (399 bp). ARE^{+} (230 bp) and ARE^{-} (148 bp) deletion segments were obtained by PCR amplification with the indicated primer pairs (see Materials and Methods). (B) Left panel, polyacrylamide gel of UV-crosslinking assays on neurosphere extracts with the ARE^{+} and ARE^{-} deletion segments. The binding activity was completely abolished in the absence of the ARE element. *Msi1* full-length 3′UTR was used as a positive control (middle lane). Right panel, UV crosslinking assay of the recombinant HuD protein with the *Msi1* 3′UTR riboprobe compared with *Gap43* as a control. The 42 kDa complex (arrowhead) can be detected. HuD specifically bound the deletion fragment ARE^{+}, but not the ARE^{-} sequence. (C) Left panel, competition experiments with the recombinant HuD protein were performed with the addition of a 100× molar excess of cold ARE^{+} and ARE^{-} riboprobes. The *Msi1*-HuD complex is shown in the first lane before the addition of the cold competitors. Right panel, an excess of cold full-length *Msi1* 3′UTR completely inhibited the formation of the mRNP complex. The antisense *Msi1* sequence (As) was not able to specifically bind HuD protein. (D) Dose-dependent binding-activity of the HuD protein (0.1, 0.2, 0.4, 1 μg) to the *Msi1* 3′UTR sequence.

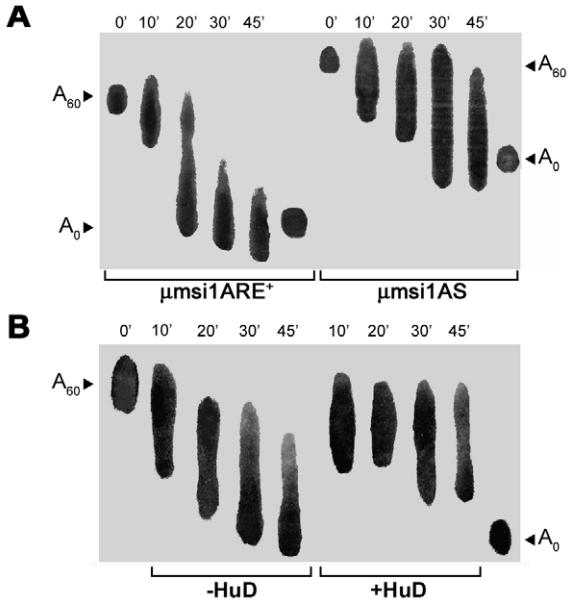

Fig. 6. The conserved ARE sequence affects *Msi1* mRNA stability in vitro. (A) Decay assay of μmsi1ARE^{+} and μmsi1AS radio-labeled transcripts at different time points. The A$_{60}$ labels represent the initial μmsi1ARE^{+} and μmsi1AS transcripts with 60 adenines in the polyA tail, whereas the A$_0$ labels represent the corresponding deadenylated transcripts. (B) The deadenylation rate of the μmsi1ARE^{+} RNA changed after the addition of 0.75 μg of the HuD protein, with a decay pattern similar to that of the μmsi1AS transcript. The deadenylation/degradation profiles were highly reproducible (compare the μmsi1ARE^{+} decay in A and B).

Journal of Cell Science

The PKCα-dependent activation of the nELAV RBPs upregulates Msi1 translation in the cytoskeleton

We have recently shown that the nELAV proteins undergo translocation from the cytosolic to the cytoskeletal compartment after treatment with phorbol esters (PMA) in human neuroblastoma SH-SY5Y cells (Pascale et al., 2005). Such translocation is accompanied by nELAV RBP threonine phosphorylation as a consequence of PKCα isozyme activation. A PKCα-dependent stabilization of the *Gap43* mRNA and an increase in its protein levels were also specifically observed in the cytoskeleton. We investigated the effect of nELAV protein activation on Msi1 content in the same cell model after treatment with PMA or solvent alone (DMSO). Msi1 protein levels were examined on cellular fractions by western blotting (Fig. 7A). PKCα translocation to the cytoskeletal compartment was clearly evident (+63%, $P<0.05$), together with nELAV protein increase (+98%, $P<0.001$), reproducing the nELAV RBP activation process already described. We also found that the Msi1 protein content significantly increased in the cytoskeleton (+107%, $P<0.001$) after nELAV RBP activation by phorbol ester treatment.

Discussion

In this paper we reveal the existence of a post-transcriptional regulatory mechanism involving Msi1 and HuD, two neural-specific RNA-binding proteins implicated in the control of the proliferation/differentiation switch during neuronal development. Msi1 overexpression has been associated with the proliferation state and degree of malignancy of brain tumors such as gliomas (Kanemura et al., 2001; Toda et al., 2001). As a consequence, we expect that Msi1 expression has to be properly regulated both at transcriptional and translational levels during the proliferation phases of neural development. We focused on the presence of a putative ARE consensus motif in *Msi1* 3′UTR gene. The high degree of conservation of the entire 3′UTR sequence in only the mammalian *Msi1* orthologs strongly suggests a putative role in a phylogenetically recent post-transcriptional regulatory mechanism. In our UV-crosslinking experiments, we found several RBPs showing a binding activity for the mouse *Msi1* 3′UTR sequence in a strictly ARE-dependent manner, in a pattern which partially overlaps the one previously described for the *Gap43* mRNA, a well-characterized target of the ELAV protein family (Chung et al., 1997; Quattrone et al., 2001). By this analogy, the common 65 kDa and 95 kDa bands could be hypothesized to correspond to the RNA-binding activities of PTB (pyrimidine-tract binding) and FBP (far-upstream-element binding) proteins, respectively (Irwin et al., 1997; Kohn et al., 1996), whereas here we demonstrate that the common 42 kDa complex does indeed represent the HuD protein. These different RBPs could play opposite roles on mRNA fate, because they were shown to bind in a competitive manner to the same cis-acting regulatory element in the *Gap43* 3′UTR sequence (Irwin et al., 1997). Moreover, it is described that the balance resulting from distinct RNA-binding activities on different regulatory elements of the same transcript may contribute to finely and gradually regulate the passage from proliferation to differentiation programs (Briata et al., 2003; Yano et al., 2005). More generally, a coordinated expression of neural genes could be obtained by the association of their mRNAs in common mRNP complexes (Keene, 2001), composed of RBPs which are temporally specified.

From our work we have an indirect evidence that nELAV activity could be developmentally regulated, because by selectively immunoprecipitating nELAV-containing mRNP complexes from adult neurospheres we were unable to show any binding to two well-known mRNA targets, *Gap43* and *Mapt*, which nonetheless are expressed in proliferating neurospheres (Esdar et al., 1999). Therefore, nELAV binding to ARE-bearing mRNAs could depend on various factors like nELAV activation and phosphorylation state (Pascale et al., 2005), and on the interaction or competition with other RBPs in a cell-state and cell-compartment specific manner.

Immunoprecipitation of neurosphere mRNPs and in vitro binding experiments with the recombinant HuD protein clearly demonstrated that nELAV proteins are able to recognize the *Msi1* transcript in an ARE-specific and ARE-dependent way. We looked for a functional meaning of this association by the approach described by Ford and Wilusz (Ford and Wilusz, 1999), a highly reproducible system that mimics the whole mRNA catabolism in vitro. Results obtained by this deadenylation and degradation assay showed that the basal decay pattern of a synthetic mRNA bearing the *Msi1* ARE sequence was faster than in its absence, and that addition of the recombinant HuD protein stabilized this transcript, as similarly described for HuB and TNF-α (Ford et al., 1999). Therefore, the HuD activity on the *Msi1* transcript suggests a positive effect on its translation, as already described for other nELAV target genes (Antic et al., 1999; Mazan-Mamczarz et al., 2003). Our functional data on neuroblastoma cells showed

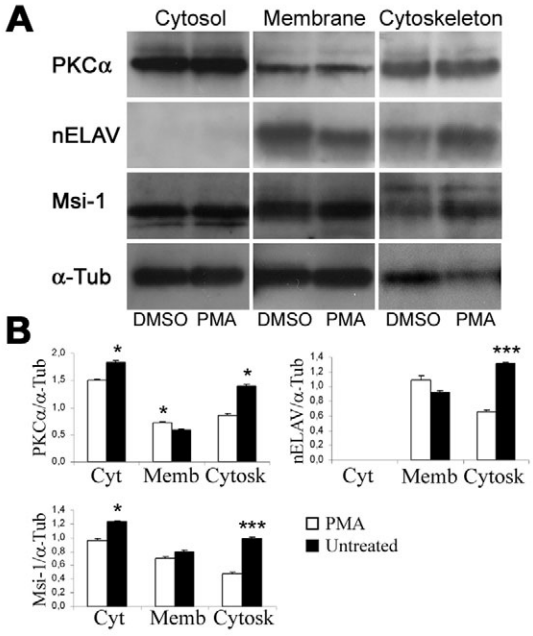

Fig. 7. nELAV-dependent upregulation of Msi1 protein after phorbol ester treatment. (A) After stimulation for 15 minutes with 100 nM PMA or DMSO, cell fractions (cytosol, membranes and cytoskeleton) were separated from human SH-SY5Y cells. Samples were analysed by western blotting with the indicated antibodies. (B) Densitometric analyses of western blot data normalized to α-tubulin protein content (mean ± s.d.; $n=3$, *$P<0.05$, ***$P<0.001$, Student's *t*-test).

Journal of Cell Science

that phorbol-ester-induced stimulation of diacylglycerol-dependent PKC isozymes determines an increase of PKCα and nELAV protein content in the cytoskeleton. This effect, previously described to be associated with PKCα and nELAV protein colocalization and with an increase in the threonine phosphorylation state of nELAV RBPs (Pascale et al., 2005), probably reflects an induction of nELAV activity at the polysomal level (A.Q., unpublished results). We showed that these phenomena were also associated with an increase in the Msi1 protein content, which was evident especially in the cytoskeletal compartment, as already shown for the nELAV protein target GAP-43.

Immunolabeling studies in cultured NSCs and in the SVZ of adult rat brains clearly showed that the nELAV RBPs are expressed and colocalize with the Msi1 protein in neural stem/progenitor cells, thus extending their biological role in NSC fate determination. This observation is in agreement with the recent description of the HuD-null mouse phenotype, where a perturbation of the proliferation and differentiation processes in neurospheres was observed (Akamatsu et al., 2005). An overall distinct and complementary expression pattern for Msi1 and nELAV RBPs has been previously reported during rodent brain development (Kaneko et al., 2000; Sakakibara et al., 1996; Sakakibara and Okano, 1997), which correlates with the observation of opposite effects of thyroid hormone on the transcription of the *Msi1* and *HuD* genes (Cuadrado et al., 2002; Cuadrado et al., 2003). However, analyzing Msi1 and nELAV protein expression in neurogenic regions, they were described to colocalize in vivo at the border of the mouse embryonic subventricular and intermediate zones (Sakakibara et al., 1996), and in differentiation-committed areas including the anterior horn of the spinal cord. Furthermore, their coexpression was also observed in vitro in MAP2-positive cells from embryonic neuroepithelial cultures (Kaneko et al., 2000).

Neurogenesis is a multi-step cell process that gradually leads a self-renewing undifferentiated NSC to acquire a completely differentiated phenotype. During embryogenesis this is achieved through symmetric division of the initial NSC, which increases the body mass as a first step. Progenitors, slightly differentiated and committed cells, originate from NSCs by sequential asymmetric division and, although for a limited number of cell cycles, they maintain the proliferative capacity. Therefore the cell programs of proliferation and differentiation are both active in progenitors, and need to be finely co-regulated. A molecular pathway known to be essential for the maintenance of actively proliferating NSCs is the Notch/Delta cascade, which controls cell division and neural differentiation (Hitoshi et al., 2002). The Msi1 protein contributes to the Notch-mediated proliferation of NSCs by binding and preventing the translation of Numb (Imai et al., 2001), which is known to negatively affect Notch activation (Cayouette and Raff, 2002; Zhong et al., 1996). On the other hand, the nELAV proteins have been widely demonstrated to be necessary and sufficient to induce neuronal differentiation in vitro. The exact timing and cascade of events that cause an NSC to completely exit from the cell cycle is hard to define, but the process is accompanied by the inactivation of cyclin-dependent kinases by specific inhibitors, such as $p21^{WAF-1}$. Interestingly, its mRNA was shown to be regulated positively by HuD (Joseph et al., 1998) which competes with hnRNP K for the same 3′UTR motif (Yano et al., 2005), and negatively by Msi1 whose binding to an adjacent site blocks $p21^{WAF-1}$ translation (Battelli et al., 2006). According to our results, we propose that the HuD-mediated stabilization of *Msi1* mRNA may serve to prolong Msi1 activity in the proliferating neural progenitor cell which is going to exit the cell cycle (Fig. 8). This would allow the stem/progenitor cell to continue to divide even after *Msi1* transcriptional inactivation.

The post-transcriptional regulative mechanism of nELAV proteins on *Msi1* mRNA seems to be evolutionarily restricted to mammals from embryonic to adult neurogenesis. Regenerative events in the SVZ have already been demonstrated to occur in vivo in the adult CNS after an ischemic insult or a damage (Douen et al., 2004; Yagita et al., 2002), whereas in the hippocampus, neurogenesis has been strictly linked to the processes of learning, neuronal plasticity and memory formation (Kempermann et al., 2004; Schinder and Gage, 2004). Upregulation and cytoskeletal translocation of nELAV proteins and the subsequent positive effects on *Gap43* mRNA levels have been recently described in tight association with synaptic plasticity and learning processes in rat dentate gyrus (Bolognani et al., 2004; Pascale et al., 2004; Quattrone et al., 2001). We speculate that our findings of a positive nELAV modulation of Msi1 transcript and protein level could be required for the transition from proliferation to differentiation of the stem/progenitor cells residing in the hippocampal subgranular zone, as well as in the SVZ. In adult

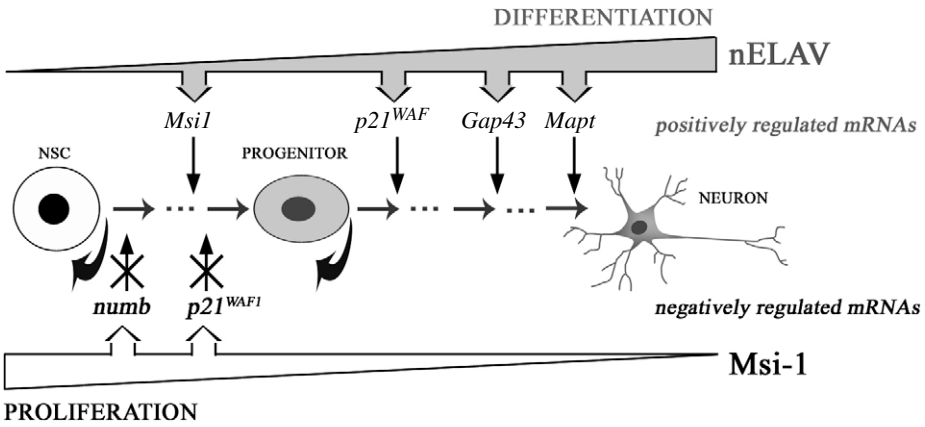

Fig. 8. Model of the hypothetical role of the nELAV RBPs during neurogenesis. In the temporal sequence of events that lead a proliferating NSC to become a differentiated neuron, Msi1 and nELAV RNA-binding activities are complementary and exert a different function on their target mRNAs. nELAV stabilization of the *Msi1* transcript may prolong its expression during the gradual passage from proliferation to differentiation.

Journal of Cell Science

neurogenic areas, nELAV activity could be assumed to be transiently induced by signals present only in restricted spatial and/or temporal conditions. We have recently demonstrated that nELAV proteins are activated by a PKCα-dependent pathway in human neuroblastoma cells (Pascale et al., 2005), and it is known that PKC-dependent signal transduction is at the basis of many aspects of CNS development (Metzger and Kapfhammer, 2003). The combination of these observations with the present results could open the possibility of a pharmacological modulation of NSC dynamics.

In conclusion, our results suggest that in mammals nELAV proteins may have a key biological role in positively regulating *Msi1* gene expression along a molecular cascade leading a proliferating stem cell towards a multi-step neural differentiation process. Since the intrinsic features of NSCs make them attractive candidates for cell-based repair therapy of the CNS (Cova et al., 2004; Lakshmipathy and Verfaillie, 2005), the nELAV/*Msi1* pathway could also represent a new pharmacological target for enhancement of neurogenesis in the treatment of neurodegenerative disorders.

Materials and Methods

Cell culture

Neural stem/progenitor cell cultures were obtained from CD1 mouse brains as previously published (Gritti et al., 1999). After isolation of adult SVZ, tissue was papain-digested and mechanically dissociated. Single cells were plated with a density of 3.5×10^3 cells/cm^2 in NS-A basal serum-free medium (Euroclone), supplemented with 20 ng/ml epidermal growth factor (EGF) and 10 ng/ml basic fibroblast growth factor (bFGF, PeproTech) and optimized for stem-cell growth. In 7-10 days neurospheres were obtained, and every 5-7 days they were dissociated to single cells for 3-5 passages in order to amplify the neural stem compartment. For immunocytochemical assays, they were plated, as neurospheres or dissociated stem/precursor cells, on an adhesive substrate (Matrigel™, Becton Dickinson) for 1 hour.

Human neuroblastoma SH-SY5Y cells were grown in MEM (Eagle's minimal essential medium) with 10% fetal calf serum, penicillin/streptomycin, non-essential amino acids and 1 mM sodium pyruvate (Invitrogen). Cells were exposed to 100 nM phorbol 12-myristate-13-acetate (PMA, Sigma) or to the solvent alone (DMSO) for 15 minutes and then the incubation was stopped with ice-cold PBS.

Protein extracts, cell fractioning and western blot

Total mouse brain and NSC cultures were homogenized in lysis buffer (150 mM NaCl, 20 mM Tris-HCl, 1% Triton X-100, protease inhibitor cocktail; Roche) and 400 U/ml RNase inhibitor (Promega). Samples were centrifuged at 12,000 ***g*** for 20 minutes at 4°C and supernatant was collected. Proteins from different cell fractions were obtained as previously published with slight modifications (Pascale et al., 1996). Briefly, SH-SY5Y cells were homogenized in buffer A (20 mM Tris-HCl pH 7.4, 2 mM EDTA, 0.5 mM EGTA, 50 mM mercaptoethanol, 0.32 mM sucrose and protease inhibitor cocktail) and centrifuged at 100,000 ***g*** for 1 hour. The supernatant containing the cytosolic fraction was collected. The pellet was resuspended in the same buffer containing 1% Triton X-100, sonicated, and incubated for 45 minutes at 4°C, then centrifuged again at 100,000 ***g*** for 1 hour. The supernatant containing the membrane fraction and the pellet with the cytoskeletal component were collected. Proteins were resolved by SDS-PAGE, transferred to nitrocellulose membranes and immunoblotted with Msi1 (1:200, Chemicon), PKCα (1:1000, Transduction Laboratories), α-tubulin (1:5000, Santa Cruz Biotechnology) antibodies, and Hu-positive serum (1:1000).

Plasmid constructs

Total RNA was extracted from whole mouse brain with TriZol® reagent (Invitrogen) and used to amplify *Msi1* and *Gap43* 3′UTR sequences by RT-PCR with the following primers: Msi1_fw TGAGGACCAGACTGAGCCAGCAAG and Msi1_rev GGGGCCTCAGTCTGCAGCAG; GAP-43_fw ATGCCTGAACTTT-AAGAAATGGCT and GAP-43_rev ATGAGGAAACAAAATGGTTTTTG. The products were cloned into pGem®-T Easy Vector (Promega). ARE$^+$ and ARE$^-$ fragments were obtained by PCR amplification of the above *Msi1*-pGem® construct with the following primers: Msi1_fw and ARE$^+$_rev GTAGGGCAA-CTGGCTAATC; ARE$^-$_fw GATTAGCCAGTTGCCCTAC and Msi1_rev. The μmsi1ARE$^+$ insert was subcloned from the *Msi1*-pGem® construct (primers: CTCATGTCTGGCTCCCCTACT and GTAGGGCAACTGGCTAATC) into the pCR®II-TOPO® (Invitrogen) vector and selected in order to have the T7 promoter at the 5′ end and the *Hin*dIII restriction site at the 3′ end of the cloning site for the mRNA decay assay. The cDNA fragment encoding the open-reading frame for HuD (GenBank accession number D31953) was amplified by RT-PCR using the following modified primers: HuD_fw TGATCTCATGAAGCCTCAGGTGTCAAATGGAC and HuD_rev CTG-CATCCCGGGGGATTTGTGGGCTTTGTTGGTT. The product was digested with *Rca*I/*Sma*I and directionally cloned into the expression vector pIVEX2.3d (Roche) with a His tag at the C-terminus. All the clones and their orientation were validated by sequencing.

RNA labeling

Radiolabeled riboprobes were obtained by transcribing 0.5 μg linearized construct DNA with 20 U T7 RNA polymerase (Roche), 20 μCi [α-^{32}P]UTP, 0.5 mM NTPs, 20 U RNase inhibitor (Promega) for 30 minutes at 37°C. The reaction was stopped at 65°C and template DNA was removed by DNaseI digestion (20 U, Roche). The resulting ^{32}P-labeled riboprobe was purified on ProbeQuant G-50 microcolumns (Amersham Biosciences).

In vitro Translation

Recombinant HuD protein was obtained in a cell-free system in which 0.5 μg HuD-pIVEX2.3d plasmid was incubated at 30°C for 6 hours in the reaction solution, containing *E. coli* lysate and amino acids according to the manufacturer's instructions (Roche). The fusion protein was purified on Ni-NTA spin kit columns and visualized by western blotting using an Anti-His$_5$ antibody (Qiagen).

UV crosslinking and immunoprecipitation

300,000 cpm of ^{32}P-labeled RNA transcripts were incubated with 40 μg of protein extract or with 300 ng of recombinant HuD protein in 15 μl ligation buffer (1.3 mM $MgCl_2$, 19 mM HEPES-KOH pH 7.4, 1.5 mM ATP, 19 mM creatine phosphate) for 10 minutes at 30°C. After addition of 5 μg tRNA, samples were irradiated with UV (Stratalinker®, Stratagene) for 5 minutes on ice and RNaseA treated (25 U) for 30 minutes. Samples were run on a 12% SDS-PAGE, and analyzed by autoradiography. For competition experiments, a 100× molar excess of cold riboprobe was added to the sample before UV irradiation. Immunoprecipitation was conducted on UV crosslinked samples by the addition of 4 μg of the selected antibody for 2 hours at 4°C. Samples were then incubated with 30 μl Protein A/G Sepharose beads (Amersham Biosciences) for 2 hours at 4°C. Immunocomplexes were then collected by centrifugation at 14,000 ***g*** for 30 seconds, washed several times in lysis buffer, run on a 12% SDS-PAGE and analyzed by autoradiography.

Immunocytochemistry and immunohistochemistry

Cells were fixed with 4% paraformaldehyde in PBS (pH 7.4) for 20 minutes, blocked with 10% normal goat serum (NGS) and permeabilized with 0.3% Triton X-100 (Gritti et al., 1999). 20-μm-thick coronal brain sections from adult rats intracardially perfused with 4% paraformaldehyde were mounted on glasses pre-coated with poly-L-lysine. Sections were boiled for 15 minutes in 50 mM Tris-HCl (pH 8.0), permeabilized with 0.5% Triton X-100 and blocked with 10% NGS. Samples were exposed to the selected antibodies overnight at 4°C (antibodies and dilutions used are specified in Table S2 in supplementary material). Slides were mounted with Fluorsave™ (Calbiochem) and acquired with a camera connected to a DMIRE2/HCS microscope (Leica Microsystems). For negative controls, the primary antibody was replaced with NGS.

Isolation and immunoprecipitation of mRNP complexes

About 5×10^6 NSCs were harvested for each condition, washed several times with cold PBS and resuspended in 1:1 (v/v) RNP buffer (100 mM KCl, 5 mM $MgCl_2$, 10 mM HEPES pH 7.4, 0.5% NP-40) (Tenenbaum et al., 2002). 50 μl protein A/G Sepharose beads, pre-coated with 8 μg of the selected antibody, were added to 300 μg NSC lysate in 1 ml NT2 buffer (50 mM Tris-HCl pH 7.4, 150 mM NaCl, 1 mM $MgCl_2$, 0.05% NP-40), containing 400 U RNase inhibitor, 1 M DTT and 20 mM EDTA. 10% of the reaction mix was collected as the initial input and RNA was extracted by TriZol® reagent (Invitrogen). After a 2-hour incubation, the immunoprecipitated mRNPs were washed several times with cold NT2 buffer, incubated with 30 μg of proteinase K for 30 minutes and phenol-chloroform extracted. After DNaseI digestion, the isolated mRNAs were retro-transcribed using SuperScriptII RT (Invitrogen), oligo dT and random primers.

Real-time quantitative PCR

Real-time PCR was performed for 45 cycles with SYBRGreen PCR Master mix (Applied Biosystems) and processed on the ABI Prism 7900HT sequence detection system. Oligonucleotide pairs for each gene were designed with Primer Express 2.0 software (Applied Biosystems) on exon boundaries. Reactions were conducted in triplicate for each sample and a dissociation curve was produced at the end. For the mRNP assays, the threshold cycle (C_t) values of immunoprecipitated samples were normalized to the C_t value of the corresponding input (ΔC_t) to account for differences in initial mRNA quantities. $\Delta\Delta C_t$ was calculated by subtracting the ΔC_t value of the sample with no antibody to the ΔC_t of the sample with anti-nELAV or anti-His$_5$ antibodies and fold differences were then expressed as $2^{-\Delta\Delta Ct}$ (Chakrabarti

et al., 2002). Statistical analysis was conducted by one-way ANOVA with Bonferroni *t*-test correction. For primer sequences and real-time PCR data see Tables S1 and S3 in supplementary material.

In vitro mRNA degradation/deadenylation assay

The mRNA decay experiments were conducted as described (Ford and Wilusz, 1999) with some modifications. Whole-brain cytoplasmic extracts were used to reproduce a neural-like environment in vitro. The addition of the polyA$_{60}$ tail to the μmsi1ARE^{+} or μmsi1AS constructs was carried out by the PCR-ligation procedure. Briefly, the double-stranded linker AGCTT(A)$_{60}$TATTTACCTCGAGCACTC was ligated to the *Hin*dIII-digested plasmids, which were then amplified with the T7 promoter primer and the complementary linker primer (GAGTGCTCGAG-GTAAATAT). Products were digested with *Ssp*I and in-vitro transcribed in the presence of 7mGpppG (Roche) and [α-^{32}P]UTP. Riboprobes were run on a denaturing 5% polyacrylamide gel (19:1) containing 8 M urea. After a short autoradiographic exposure, bands were excized from the gel, eluted overnight in HSCB buffer (400 mM NaCl, 25 mM Tris-HCl pH 7.6, 0.1% SDS), phenol-chloroform extracted and ethanol precipitated. 200,000 cpm riboprobes were incubated with 200 μg of mouse brain extract and 0.5 μg polyA (Amersham Biosciences) in 15 μl deadenylation buffer (2.6% polyvinyl alcohol, 1 mM ATP, 13 mM creatine phosphate) at 30°C. At the indicated time intervals reactions were stopped with 400 μl HSCB buffer. RNA was extracted in phenol-chloroform, separated on an urea-denatured 5% polyacrylamide gel and visualized by autoradiography.

We thank C. Fenoglio, A. Grifa and M. G. Savino for their kind help. This work was supported by Italian Ministry of Health (Mal. Neurodegenerative, ex art.56 Anno 2003), Fondazione I.Monzino and Fondazione FiorGen.

References

Abe, R., Sakashita, E., Yamamoto, K. and Sakamoto, H. (1996). Two different RNA binding activities for the AU-rich element and the poly(A) sequence of the mouse neuronal protein mHuC. *Nucleic Acids Res.* **24**, 4895-4901.

Akamatsu, W., Okano, H. J., Osumi, N., Inoue, T., Nakamura, S., Sakakibara, S., Miura, M., Matsuo, N., Darnell, R. B. and Okano, H. (1999). Mammalian ELAV-like neuronal RNA-binding proteins HuB and HuC promote neuronal development in both the central and the peripheral nervous systems. *Proc. Natl. Acad. Sci. USA* **96**, 9885-9890.

Akamatsu, W., Fujihara, H., Mitsuhashi, T., Yano, M., Shibata, S., Hayakawa, Y., Okano, H. J., Sakakibara, S., Takano, H., Takano, T. et al. (2005). The RNA-binding protein HuD regulates neuronal cell identity and maturation. *Proc. Natl. Acad. Sci. USA* **102**, 4625-4630.

Alvarez-Buylla, A. and Garcia-Verdugo, J. M. (2002). Neurogenesis in adult subventricular zone. *J. Neurosci.* **22**, 629-634.

Antic, D. and Keene, J. D. (1997). Embryonic lethal abnormal visual RNA-binding proteins involved in growth, differentiation, and posttranscriptional gene expression. *Am. J. Hum. Genet.* **61**, 273-278.

Antic, D., Lu, N. and Keene, J. D. (1999). ELAV tumor antigen, Hel-N1, increases translation of neurofilament M mRNA and induces formation of neurites in human teratocarcinoma cells. *Genes Dev.* **13**, 449-461.

Aranda-Abreu, G. E., Behar, L., Chung, S., Furneaux, H. and Ginzburg, I. (1999). Embryonic lethal abnormal vision-like RNA-binding proteins regulate neurite outgrowth and tau expression in PC12 cells. *J. Neurosci.* **19**, 6907-6917.

Asson-Batres, M. A., Spurgeon, S. L., Diaz, J., DeLoughery, T. G. and Bagby, G. C., Jr (1994). Evolutionary conservation of the AU-rich 3′ untranslated region of messenger RNA. *Proc. Natl. Acad. Sci. USA* **91**, 1318-1322.

Bakheet, T., Frevel, M., Williams, B. R., Greer, W. and Khabar, K. S. (2001). ARED: human AU-rich element-containing mRNA database reveals an unexpectedly diverse functional repertoire of encoded proteins. *Nucleic Acids Res.* **29**, 246-254.

Barami, K., Iversen, K., Furneaux, H. and Goldman, S. A. (1995). Hu protein as an early marker of neuronal phenotypic differentiation by subependymal zone cells of the adult songbird forebrain. *J. Neurobiol.* **28**, 82-101.

Battelli, C., Nikopoulos, G. N., Mitchell, J. G. and Verdi, J. M. (2006). The RNA-binding protein Musashi-1 regulates neural development through the translational repression of p21(WAF-1). *Mol. Cell Neurosci.* **31**, 85-96.

Bevilacqua, A., Ceriani, M. C., Capaccioli, S. and Nicolin, A. (2003). Post-transcriptional regulation of gene expression by degradation of messenger RNAs. *J. Cell. Physiol.* **195**, 356-372.

Bez, A., Corsini, E., Curti, D., Biggiogera, M., Colombo, A., Nicosia, R. F., Pagano, S. F. and Parati, E. A. (2003). Neurosphere and neurosphere-forming cells: morphological and ultrastructural characterization. *Brain Res.* **993**, 18-29.

Bolognani, F., Merhege, M. A., Twiss, J. and Perrone-Bizzozero, N. I. (2004). Dendritic localization of the RNA-binding protein HuD in hippocampal neurons: association with polysomes and upregulation during contextual learning. *Neurosci. Lett.* **371**, 152-157.

Bottai, D., Fiocco, R., Gelain, F., Defilippis, L., Galli, R., Gritti, A. and Vescovi, L. A. (2003). Neural stem cells in the adult nervous system. *J. Hematother. Stem Cell Res.* **12**, 655-670.

Briata, P., Ilengo, C., Corte, G., Moroni, C., Rosenfeld, M. G., Chen, C. Y. and Gherzi, R. (2003). The Wnt/beta-catenin–>Pitx2 pathway controls the turnover of Pitx2 and other unstable mRNAs. *Mol. Cell* **12**, 1201-1211.

Cayouette, M. and Raff, M. (2002). Asymmetric segregation of Numb: a mechanism for neural specification from Drosophila to mammals. *Nat. Neurosci.* **5**, 1265-1269.

Chakrabarti, S. K., James, J. C. and Mirmira, R. G. (2002). Quantitative assessment of gene targeting in vitro and in vivo by the pancreatic transcription factor, Pdx1. Importance of chromatin structure in directing promoter binding. *J. Biol. Chem.* **277**, 13286-13293.

Chen, C. Y. and Shyu, A. B. (1995). AU-rich elements: characterization and importance in mRNA degradation. *Trends Biochem. Sci.* **20**, 465-470.

Chu, E., Koeller, D. M., Casey, J. L., Drake, J. C., Chabner, B. A., Elwood, P. C., Zinn, S. and Allegra, C. J. (1991). Autoregulation of human thymidylate synthase messenger RNA translation by thymidylate synthase. *Proc. Natl. Acad. Sci. USA* **88**, 8977-8981.

Chung, S., Eckrich, M., Perrone-Bizzozero, N., Kohn, D. T. and Furneaux, H. (1997). The Elav-like proteins bind to a conserved regulatory element in the 3′-untranslated region of GAP-43 mRNA. *J. Biol. Chem.* **272**, 6593-6598.

Cova, L., Ratti, A., Volta, M., Fogh, I., Cardin, V., Corbo, M. and Silani, V. (2004). Stem cell therapy for neurodegenerative diseases: the issue of transdifferentiation. *Stem Cells Dev.* **13**, 121-131.

Cuadrado, A., Garcia-Fernandez, L. F., Imai, T., Okano, H. and Munoz, A. (2002). Regulation of tau RNA maturation by thyroid hormone is mediated by the neural RNA-binding protein musashi-1. *Mol. Cell. Neurosci.* **20**, 198-210.

Cuadrado, A., Navarro-Yubero, C., Furneaux, H. and Munoz, A. (2003). Neuronal HuD gene encoding a mRNA stability regulator is transcriptionally repressed by thyroid hormone. *J. Neurochem.* **86**, 763-773.

Ding, Y., Chan, C. Y. and Lawrence, C. E. (2004). Sfold web server for statistical folding and rational design of nucleic acids. *Nucleic Acids Res.* **32**, W135-W141.

Douen, A. G., Dong, L., Vanance, S., Munger, R., Hogan, M. J., Thompson, C. S. and Hakim, A. M. (2004). Regulation of nestin expression after cortical ablation in adult rat brain. *Brain Res.* **1008**, 139-146.

Esdar, C., Oehrlein, S. A., Reinhardt, S., Maelicke, A. and Herget, T. (1999). The protein kinase C (PKC) substrate GAP-43 is already expressed in neural precursor cells, colocalizes with PKCeta and binds calmodulin. *Eur. J. Neurosci.* **11**, 503-516.

Ford, L. P. and Wilusz, J. (1999). An in vitro system using HeLa cytoplasmic extracts that reproduces regulated mRNA stability. *Methods* **17**, 21-27.

Ford, L. P., Watson, J., Keene, J. D. and Wilusz, J. (1999). ELAV proteins stabilize deadenylated intermediates in a novel in vitro mRNA deadenylation/degradation system. *Genes Dev.* **13**, 188-201.

Galli, R., Gritti, A., Bonfanti, L. and Vescovi, A. L. (2003). Neural stem cells: an overview. *Circ. Res.* **92**, 598-608.

Gao, F. B., Carson, C. C., Levine, T. and Keene, J. D. (1994). Selection of a subset of mRNAs from combinatorial 3′ untranslated region libraries using neuronal RNA-binding protein Hel-N1. *Proc. Natl. Acad. Sci. USA* **91**, 11207-11211.

Gritti, A., Frolichsthal-Schoeller, P., Galli, R., Parati, E. A., Cova, L., Pagano, S. F., Bjornson, C. R. and Vescovi, A. L. (1999). Epidermal and fibroblast growth factors behave as mitogenic regulators for a single multipotent stem cell-like population from the subventricular region of the adult mouse forebrain. *J. Neurosci.* **19**, 3287-3297.

Hitoshi, S., Alexson, T., Tropepe, V., Donoviel, D., Elia, A. J., Nye, J. S., Conlon, R. A., Mak, T. W., Bernstein, A. and van der Kooy, D. (2002). Notch pathway molecules are essential for the maintenance, but not the generation, of mammalian neural stem cells. *Genes Dev.* **16**, 846-858.

Imai, T., Tokunaga, A., Yoshida, T., Hashimoto, M., Mikoshiba, K., Weinmaster, G., Nakafuku, M. and Okano, H. (2001). The neural RNA-binding protein Musashi1 translationally regulates mammalian numb gene expression by interacting with its mRNA. *Mol. Cell. Biol.* **21**, 3888-3900.

Irwin, N., Baekelandt, V., Goritchenko, L. and Benowitz, L. I. (1997). Identification of two proteins that bind to a pyrimidine-rich sequence in the 3′-untranslated region of GAP-43 mRNA. *Nucleic Acids Res.* **25**, 1281-1288.

Joseph, B., Orlian, M. and Furneaux, H. (1998). p21(waf1) mRNA contains a conserved element in its 3′-untranslated region that is bound by the Elav-like mRNA-stabilizing proteins. *J. Biol. Chem.* **273**, 20511-20516.

Kaneko, Y., Sakakibara, S., Imai, T., Suzuki, A., Nakamura, Y., Sawamoto, K., Ogawa, Y., Toyama, Y., Miyata, T. and Okano, H. (2000). Musashi1: an evolutionally conserved marker for CNS progenitor cells including neural stem cells. *Dev. Neurosci.* **22**, 139-153.

Kanemura, Y., Mori, K., Sakakibara, S., Fujikawa, H., Hayashi, H., Nakano, A., Matsumoto, T., Tamura, K., Imai, T., Ohnishi, T. et al. (2001). Musashi1, an evolutionarily conserved neural RNA-binding protein, is a versatile marker of human glioma cells in determining their cellular origin, malignancy, and proliferative activity. *Differentiation* **68**, 141-152.

Kasashima, K., Terashima, K., Yamamoto, K., Sakashita, E. and Sakamoto, H. (1999). Cytoplasmic localization is required for the mammalian ELAV-like protein HuD to induce neuronal differentiation. *Genes Cells* **4**, 667-683.

Kee, N., Sivalingam, S., Boonstra, R. and Wojtowicz, J. M. (2002). The utility of Ki-67 and BrdU as proliferative markers of adult neurogenesis. *J. Neurosci. Methods* **115**, 97-105.

Keene, J. D. (2001). Ribonucleoprotein infrastructure regulating the flow of genetic information between the genome and the proteome. *Proc. Natl. Acad. Sci. USA* **98**, 7018-7024.

Kempermann, G., Jessberger, S., Steiner, B. and Kronenberg, G. (2004). Milestones of neuronal development in the adult hippocampus. *Trends Neurosci.* **27**, 447-452.

Kohn, D. T., Tsai, K. C., Cansino, V. V., Neve, R. L. and Perrone-Bizzozero, N. I.

Journal of Cell Science

(1996). Role of highly conserved pyrimidine-rich sequences in the 3′ untranslated region of the GAP-43 mRNA in mRNA stability and RNA-protein interactions. *Brain Res. Mol. Brain Res.* **36**, 240-250.

Lakshmipathy, U. and Verfaillie, C. (2005). Stem cell plasticity. *Blood Rev.* **19**, 29-38.

Lal, A., Mazan-Mamczarz, K., Kawai, T., Yang, X., Martindale, J. L. and Gorospe, M. (2004). Concurrent versus individual binding of HuR and AUF1 to common labile target mRNAs. *EMBO J.* **23**, 3092-3102.

Levine, T. D., Gao, F., King, P. H., Andrews, L. G. and Keene, J. D. (1993). Hel-N1: an autoimmune RNA-binding protein with specificity for 3′ uridylate-rich untranslated regions of growth factor mRNAs. *Mol. Cell. Biol.* **13**, 3494-3504.

Marusich, M. F., Furneaux, H. M., Henion, P. D. and Weston, J. A. (1994). Hu neuronal proteins are expressed in proliferating neurogenic cells. *J. Neurobiol.* **25**, 143-155.

Maslov, A. Y., Barone, T. A., Plunkett, R. J. and Pruitt, S. C. (2004). Neural stem cell detection, characterization, and age-related changes in the subventricular zone of mice. *J. Neurosci.* **24**, 1726-1733.

Mazan-Mamczarz, K., Galban, S., Lopez de Silanes, I., Martindale, J. L., Atasoy, U., Keene, J. D. and Gorospe, M. (2003). RNA-binding protein HuR enhances p53 translation in response to ultraviolet light irradiation. *Proc. Natl. Acad. Sci. USA* **100**, 8354-8359.

Metzger, F. and Kapfhammer, J. P. (2003). Protein kinase C: its role in activity-dependent Purkinje cell dendritic development and plasticity. *Cerebellum* **2**, 206-214.

Morshead, C. M. and van der Kooy, D. (2004). Disguising adult neural stem cells. *Curr. Opin. Neurobiol.* **14**, 125-131.

Nakamura, M., Okano, H., Blendy, J. A. and Montell, C. (1994). Musashi, a neural RNA-binding protein required for Drosophila adult external sensory organ development. *Neuron* **13**, 67-81.

Okano, H. J. and Darnell, R. B. (1997). A hierarchy of Hu RNA binding proteins in developing and adult neurons. *J. Neurosci.* **17**, 3024-3037.

Okano, H., Imai, T. and Okabe, M. (2002). Musashi: a translational regulator of cell fate. *J. Cell Sci.* **115**, 1355-1359.

Pascale, A., Fortino, I., Govoni, S., Trabucchi, M., Wetsel, W. C. and Battaini, F. (1996). Functional impairment in protein kinase C by RACK1 (receptor for activated C kinase 1) deficiency in aged rat brain cortex. *J. Neurochem.* **67**, 2471-2477.

Pascale, A., Gusev, P. A., Amadio, M., Dottorini, T., Govoni, S., Alkon, D. L. and Quattrone, A. (2004). Increase of the RNA-binding protein HuD and posttranscriptional up-regulation of the GAP-43 gene during spatial memory. *Proc. Natl. Acad. Sci. USA* **101**, 1217-1222.

Pascale, A., Amadio, M., Scapagnini, G., Lanni, C., Racchi, M., Provenzani, A., Govoni, S., Alkon, D. L. and Quattrone, A. (2005). Neuronal ELAV proteins enhance mRNA stability by a PKCalpha-dependent pathway. *Proc. Natl. Acad. Sci. USA* **102**, 12065-12070.

Perrone-Bizzozero, N. and Bolognani, F. (2002). Role of HuD and other RNA-binding proteins in neural development and plasticity. *J. Neurosci. Res.* **68**, 121-126.

Qian, X., Shen, Q., Goderie, S. K., He, W., Capela, A., Davis, A. A. and Temple, S. (2000). Timing of CNS cell generation: a programmed sequence of neuron and glial cell production from isolated murine cortical stem cells. *Neuron* **28**, 69-80.

Quattrone, A., Pascale, A., Nogues, X., Zhao, W., Gusev, P., Pacini, A. and Alkon, D. L. (2001). Posttranscriptional regulation of gene expression in learning by the neuronal ELAV-like mRNA-stabilizing proteins. *Proc. Natl. Acad. Sci. USA* **98**, 11668-11673.

Robinow, S. and White, K. (1991). Characterization and spatial distribution of the ELAV protein during Drosophila melanogaster development. *J. Neurobiol.* **22**, 443-461.

Roegiers, F. and Jan, Y. N. (2004). Asymmetric cell division. *Curr. Opin. Cell Biol.* **16**, 195-205.

Sakakibara, S. and Okano, H. (1997). Expression of neural RNA-binding proteins in the postnatal CNS: implications of their roles in neuronal and glial cell development. *J. Neurosci.* **17**, 8300-8312.

Sakakibara, S., Imai, T., Hamaguchi, K., Okabe, M., Aruga, J., Nakajima, K., Yasutomi, D., Nagata, T., Kurihara, Y., Uesugi, S. et al. (1996). Mouse-Musashi-1, a neural RNA-binding protein highly enriched in the mammalian CNS stem cell. *Dev. Biol.* **176**, 230-242.

Sakakibara, S., Nakamura, Y., Satoh, H. and Okano, H. (2001). Rna-binding protein Musashi2: developmentally regulated expression in neural precursor cells and subpopulations of neurons in mammalian CNS. *J. Neurosci.* **21**, 8091-8107.

Samson, M. L. (1998). Evidence for 3′ untranslated region-dependent autoregulation of the Drosophila gene encoding the neuronal nuclear RNA-binding protein ELAV. *Genetics* **150**, 723-733.

Schaeffer, C., Bardoni, B., Mandel, J. L., Ehresmann, B., Ehresmann, C. and Moine, H. (2001). The fragile X mental retardation protein binds specifically to its mRNA via a purine quartet motif. *EMBO J.* **20**, 4803-4813.

Schinder, A. F. and Gage, F. H. (2004). A hypothesis about the role of adult neurogenesis in hippocampal function. *Physiology (Bethesda)* **19**, 253-261.

Shaw, G. and Kamen, R. (1986). A conserved AU sequence from the 3′ untranslated region of GM-CSF mRNA mediates selective mRNA degradation. *Cell* **46**, 659-667.

Suslov, O. N., Kukekov, V. G., Ignatova, T. N. and Steindler, D. A. (2002). Neural stem cell heterogeneity demonstrated by molecular phenotyping of clonal neurospheres. *Proc. Natl. Acad. Sci. USA* **99**, 14506-14511.

Szabo, A., Dalmau, J., Manley, G., Rosenfeld, M., Wong, E., Henson, J., Posner, J. B. and Furneaux, H. M. (1991). HuD, a paraneoplastic encephalomyelitis antigen, contains RNA-binding domains and is homologous to Elav and Sex-lethal. *Cell* **67**, 325-333.

Tenenbaum, S. A., Lager, P. J., Carson, C. C. and Keene, J. D. (2002). Ribonomics: identifying mRNA subsets in mRNP complexes using antibodies to RNA-binding proteins and genomic arrays. *Methods* **26**, 191-198.

Toda, M., Iizuka, Y., Yu, W., Imai, T., Ikeda, E., Yoshida, K., Kawase, T., Kawakami, Y., Okano, H. and Uyemura, K. (2001). Expression of the neural RNA-binding protein Musashi1 in human gliomas. *Glia* **34**, 1-7.

Wakamatsu, Y. and Weston, J. A. (1997). Sequential expression and role of Hu RNA-binding proteins during neurogenesis. *Development* **124**, 3449-3460.

Wiese, C., Rolletschek, A., Kania, G., Blyszczuk, P., Tarasov, K. V., Tarasova, Y., Wersto, R. P., Boheler, K. R. and Wobus, A. M. (2004). Nestin expression–a property of multi-lineage progenitor cells? *Cell. Mol. Life Sci.* **61**, 2510-2522.

Yagita, Y., Kitagawa, K., Sasaki, T., Miyata, T., Okano, H., Hori, M. and Matsumoto, M. (2002). Differential expression of Musashi1 and nestin in the adult rat hippocampus after ischemia. *J. Neurosci. Res.* **69**, 750-756.

Yano, M., Okano, H. J. and Okano, H. (2005). Involvement of Hu and heterogeneous nuclear ribonucleoprotein K in neuronal differentiation through p21 mRNA post-transcriptional regulation. *J. Biol. Chem.* **280**, 12690-12699.

Zhong, W., Feder, J. N., Jiang, M. M., Jan, L. Y. and Jan, Y. N. (1996). Asymmetric localization of a mammalian numb homolog during mouse cortical neurogenesis. *Neuron* **17**, 43-53.

Journal of Cell Science

Accepted 21 December 2005
Journal of Cell Science 119, 1442-1452 Published by The Company of Biologists 2006
doi:10.1242/jcs.02852

Supplementary Tables

Table S1. Real-time PCR data

Gene	Sample	Mean C_t	ΔC_t	$\Delta\Delta C_t$	Fold Difference ($2^{-\Delta\Delta Ct}$)	s.e.m.
Rpl10a	Input_nELAV	18.8	8.6	-1.7	3.2	1.7
	IP_nELAV	27.4				
	Input_His5	18.6	9.2	-0.9	1.9	0.6
	IP_His5	27.8				
	Input_noAb	19.2	10.3	0	1.0	0
	IP_noAb	29.5				
Msi-1	Input_nELAV	25.9	1.7	-6.0	64	7.9
	IP_nELAV	27.6				
	Input_His5	25.4	6.7	-1.0	2.0	2.5
	IP_His5	32.2				
	Input_noAb	26.4	7.7	0	1.0	0
	IP_noAb	34.1				
GAP-43	Input_nELAV	22.3	7.1	-1.1	2.1	0.8
	IP_nELAV	29.3				
	Input_His5	21.9	7.8	-0.4	1.3	0.9
	IP_His5	29.7				
	Input_noAb	22.8	8.2	0	1.0	0
	IP_noAb	31				
Tau	Input_nELAV	27	9.0	-2.0	4.0	1.4
	IP_nELAV	35.1				
	Input_His5	26	9.9	-1.1	2.1	3.0
	IP_His5	35.9				
	Input_noAb	27.1	11	0	1	0
	IP_noAb	38.1				

Table S2. Antibody dilutions in ICC and IHC assays

Musashi-1	Polyclonal	Chemicon	1:100 for ICC and 1:150 for IHC
nELAV (16A11)	Monoclonal	Molecular Probes	1:100 for ICC and 1:200 for IHC
Ki67	Polyclonal	NovoCastra	1:500 for ICC and 1:600 for IHC
Nestin	Monoclonal/Polyclonal	Chemicon	1:200 for ICC
Secondary antibody Cy2	Monoclonal/Polyclonal	Jackson ImmunoRes. Lab.	1:500 for ICC and IHC
Secondary antibody Cy3	Monoclonal/Polyclonal	Jackson ImmunoRes. Lab.	1:500 for ICC and IHC

Table S3. Primer sequences for real-time PCR

Msi-1_fw	TGCAGCTGACTGAGGACCAGA
Msi-1_rev	GGTGTCCCAATCCCCT
GAP-43_fw	AGGCTGACCAAGAACATGCCT
GAP-43_rev	GGCAACGTGGAAAGCCATTT
Rpl10a_fw	GAAGAAGGTGCTGTGTTTGGC
Rpl10a_rev	TCGGTCATCTTCACGTGGC
Tau_for	TCCCTGGAGGAGGGAATAAGA
Tau_rev	CCCTGAAGGTCAGCTTGTGG